EUROPEAN SYNCHROTRON RADIATION FACILITY

INSTALLATION EUROPEENNE DE RAYONNEMENT SYNCHROTRON

ESRF

Experiment Report Form

The double page inside this form is to be filled in by all users or groups of users who have had access to beam time for measurements at the ESRF.

Once completed, the report should be submitted electronically to the User Office using the **Electronic Report Submission Application:**

http://193.49.43.2:8080/smis/servlet/UserUtils?start

Reports supporting requests for additional beam time

Reports can now be submitted independently of new proposals – it is necessary simply to indicate the number of the report(s) supporting a new proposal on the proposal form.

The Review Committees reserve the right to reject new proposals from groups who have not reported on the use of beam time allocated previously.

Reports on experiments relating to long term projects

Proposers awarded beam time for a long term project are required to submit an interim report at the end of each year, irrespective of the number of shifts of beam time they have used.

Published papers

All users must give proper credit to ESRF staff members and proper mention to ESRF facilities which were essential for the results described in any ensuing publication. Further, they are obliged to send to the Joint ESRF/ ILL library the complete reference and the abstract of all papers appearing in print, and resulting from the use of the ESRF.

Should you wish to make more general comments on the experiment, please note them on the User Evaluation Form, and send both the Report and the Evaluation Form to the User Office.

Deadlines for submission of Experimental Reports

- 1st March for experiments carried out up until June of the previous year;
- 1st September for experiments carried out up until January of the same year.

Instructions for preparing your Report

- fill in a separate form for each project or series of measurements.
- type your report, in English.
- include the reference number of the proposal to which the report refers.
- make sure that the text, tables and figures fit into the space available.
- if your work is published or is in press, you may prefer to paste in the abstract, and add full reference details. If the abstract is in a language other than English, please include an English translation.

ESRF	**Experiment title:** Materials Science Applications of a 3-dimensional x-ray microscope	**Experiment number**: HS-968
Beamline:	**Date of experiment**: from: 1/9 1999 to: 1/9 2001	**Date of report**: 1/3/2002
Shifts:	**Local contact(s)**: U. Lienert, S. Grigull	*Received at ESRF:*

Names and affiliations of applicants (* indicates experimentalists):

H.F. Poulsen*, L. Margulies*, S. Schmidt*, E.M. Lauridsen*, S.F. Nielsen*, T. Lorentzen*, D. Juul Jensen, G. Winther, L.G. Andersen*, Materials Research Dept., DK-4000 Roskilde.

R.M. Suter, Dept. of Physics, Carnegie Mellon University, Pittsburgh, PA 15213 USA.

U. Lienert, ESRF

Report: In this final report we summarize the major experimental results obtained using the 3DXRD microscope under longterm proposal HS-968. This has included the development and validation of the tracking technique, demonstrated here for 3D grain mapping and strain tensor measurement of individual grains. The application on the instrument towards problems in ceramic materials is shown in studies on high T_c superconductors, and a validation study on Al_2O_3 demonstrating for the first time the ability to perform structural refinement of individual grains within a bulk polycrystal. Finally, we demonstrate the potential of the 3DXRD for following the kinetics of sub-micron structures during annealing processes.

Establishment of the tracking technique

A non-destructive technique for fast and complete three dimensional mapping of the volumes, morphologies, orientations and strain-states of individual grains in coarse-grained polycrystalline materials (metals, ceramics, minerals) has been developed[8,9]. Based on the 3DXRD microscope the technique utilises a monochromatic beam of hard x-rays focused into a line and a two-dimensional detector. An x-ray tracing algorithm is employed, inspired by the use of three-dimensional detectors in high-energy physics.

3D grain mapping

To obtain the cross-sectional grain shape, the periphery of the diffraction spot in the image acquired at the closest distance is projected into the illuminated sample plane along the direction determined by the fit (see Fig.1). This procedure is repeated for a number of ω settings, producing a complete map of all grain boundaries and grain orientations in the plane. (The strain-state may be derived simultaneously from a second CCD placed at large distances - the one used here is semi-transparent).

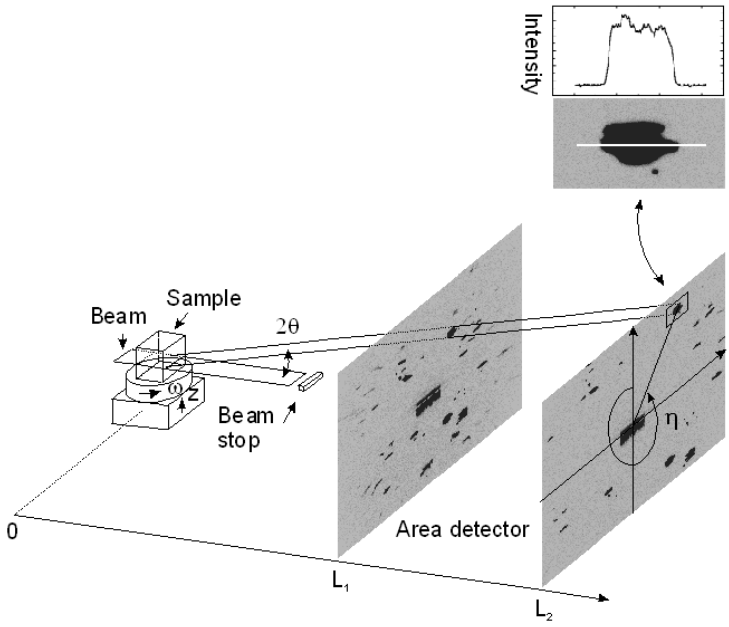

Fig. 1. The line-focus defines a layer within the sample. All grains that happen to fulfil Bragg's conditions in this layer will give rise to a diffraction spot on the detector. The position of each diffraction spot is measured. During the exposure, the sample is oscillated over a range $\Delta\omega$ (depending on the mosaic spread of the grain) to obtain a complete integration of the Bragg intensity. The intensity weighted centre-of-mass (CM) of each diffraction spot is computed. This procedure is repeated at several detector distances corresponding to different L values. Linear fits through corresponding CM points extrapolate to the CM of the diffracting grains and also yield the angles 2θ and η.

To demonstrate the efficacy of the technique a coarse-grained 99.996% pure aluminium sample was investigated. Initially the grains at a sample surface were mapped by electron microscopy (EBSP), and found to have an average mosaic spread of 1 degree. The sample was aligned with the same surface parallel to the beam at the 3DXRD microscope and the tracing procedure was performed with a 5 µm wide beam incident just below the surface. With 1 second exposure time, 22 ω-settings with $\Delta\omega = 2$ degrees and *L = 7.5, 10.3* and *13* mm, the total data acquisition time was less than 2 minutes.

The grain orientations determined by the EBSP and the tracking technique reproduced within the combined alignment errors of the set-ups. The resulting grain boundaries are superposed in figure 2, where colours and black outlines mark the grains and grain boundaries on the surface of an Aluminium polycrystal as determined by electron microscopy (EBSP). Superposed, as white lines are the grain boundaries resulting from the synchrotron experiment. The 3DXRD boundaries are raw data with no interpolation or averaging between reflections from the same or neighbouring grains. Complete three-dimensional maps over cubic-millimetres of material can then be obtained within ~1 h simply by translating the sample in *z* and repeating the procedure for several layers.

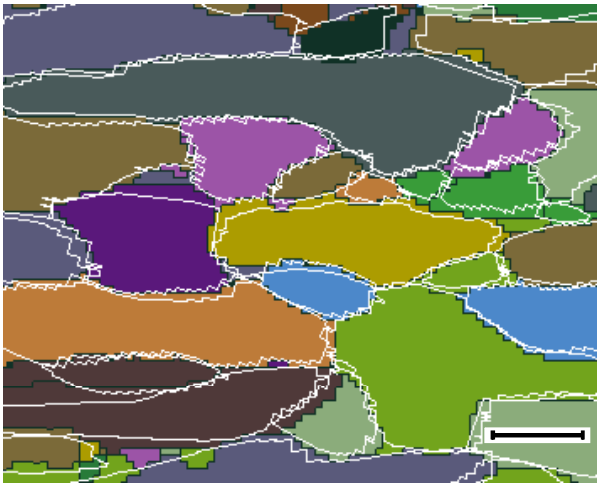

Fig. 2. The white lines superimposed are the grain boundaries resulting from the X-ray tracking. The scale bar at the bottom is 400 µm.

Strain Tensor Development of an Interior Single Grain in a Polycrystal Under Loading

By using a large area detector (FRELON coupled with an image intensifier) far from the sample, sufficient angular resolution may be obtained to allow the determination of strain tensor components of individual grains as a function of applied load. As in the 3D grain mapping case, the software package GRAINDEX[8] is used to sort reflections by their grain of origin. In this case 17 reflections were followed and fit using an over determined set of equations for the full strain tensor. The estimated error on the strain is 1 x 10^{-4} [9]. The over determined set of equation should allow for the simultaneous fitting of the grain offsets from the center rotation, which will allow future experiments to measure large ensemble of grains simultaneously. This will provide the needed statistics to explore issues relevant to the strength of local grain interaction.

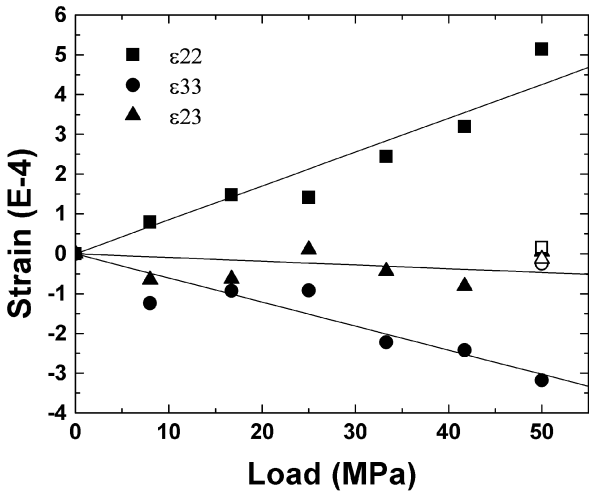

Fig. 3. Evolution of selected strain components for an embedded Cu grain during tensile deformation. ε_{22} (■) and ε_{33} (•) represent directions along the tensile axis and transverse to it, respectively. ε_{23} (▲) is the associated shear component. Lines represent linear fits to the data. Open symbols are values measured after unloading.

In-situ Study of Individual Grains in Superconducting BSCCO/Ag Tapes using the 3DXRD Microscope

With the 3DXRD microscope we aimed at following the kinetics of the individual embedded grains inside a Ag clad BSCCO High T_c superconducting tape during heating and 12 hours of annealing at 838 °C. An 80 keV beam was focused to a 5 μm horizontal line, and limited horizontally to 40 μm by a slit. The diffracted beam from a single filament green tape was monitored by a CCD camera while oscillating the tape by 0.5°. Reflections from individual grains of the main phases: 2212 ($Bi_{2-x}Pb_xSr_2CaCu_2O_y$) and 2223 ($Bi_{2-x}Pb_xSr_2Ca_2Cu_3O_y$) are clearly visible as dots on the detector. The grain volume is proportional to the integrated intensity of the dots and the grain stoichiometry related to the 2Θ angle. Due to identical a/b- axes the transformation of 2212 to 2223 will give rise to spots appearing with identical azimuthal angle in the images, if and only if the grain orientation is conserved. In this way essential information on the transformation mechanism should be available ("intercalation" vs. "growth on top" vs. "random nucleation"). At the beginning of the annealing the diffraction pattern consisted of segmented Debye-Scherrer powder rings. At 825 °C the diffraction spots from grains appeared. Validation tests were made continuously to test whether the full integrated intensity was monitored.

The prospect arising from this experiment leads beyond high Tc superconductivity. With the 3DXRD microscope it will in general be feasible to perform statistics on the volumes, strains, stoichiometry and orientation of the embedded grains in a powder, provided the grain volumes are a few μm^3.

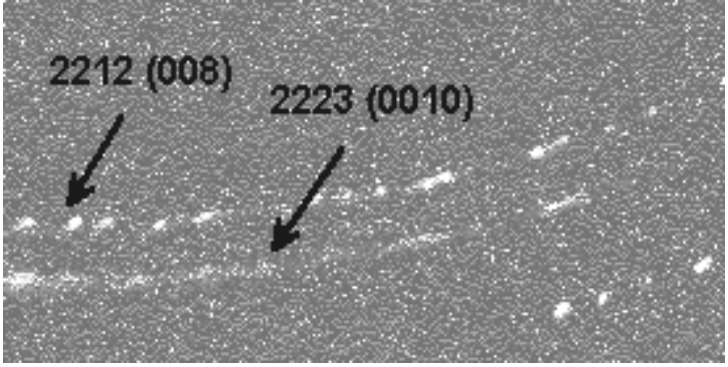

Fig. 4. Detail of image acquired after 11.5 hours of annealing at 838 °C in air. Dots appearing on the (008) and (0010) Debye Scherrer rings associated with the 2212 and 2223 phases, reflect the transformation from 2212 to 2223.[5]

Structural refinement of Individual Grains within Polycrystals

A method has been developed for simultaneous structural refinement of up to several hundred grains inside powders or polycrystals[15]. The method is based on the use of hard x-rays and the indexing program GRAINDEX[8], where grain orientations are found by scanning in Euler space. Conventional experimental set-ups and refinement programs for single crystal work can be applied. The method is validated by a study of a sintered plate of Al_2O_3, containing on the order of 1500 grains in the gauge volume.

In order to characterize the global data quality, a pseudo-powder pattern was generated by summing together all of the rotation photographs. The pixel by pixel median values were then subtracted – this procedure serves to remove the background (mostly air scattering) from the pattern, as the median image contains only the ubiquitous part of the data, eliminating outliers (diffraction spots). This difference image was then azimuthially integrated, and 10 parameters (2 lattice parameters, 2 atomic coordinates, 2 isotropic atomic displacement parameters, 3 peak shape parameters and scale factor) were refined against the resulting powder pattern using Fullprof. The results of the Rietveld refinement are given in the table below. First the weighted mean and median of the values obtained from 57 independent grains are listed, then values from the best grain, followed by values arising from merging all data from the 17 largest grains into a single data set, and the result of a conventional Rietveld refinement. At the end is listed single crystal reference values from 3 articles.

	Al z		O x		Al u (Å^2)		O u (Å^2)	
Grain Median	0.35221		0.30527		0.0032		0.0010	
Grain Wt. Mean	0.35203	(11)	0.3071	(6)	0.0048	(7)	0.0046	(5)
Best Grain	0.35197	(13)	0.3072	(11)	0.0041	(8)	0.0048	(13)
Full Data Set	0.35220	(29)	0.3060	(15)	0.0038	(10)	0.0012	(17)
Treated as Powder	0.35060	(40)	0.3094	(13)	0.057	(12)	0.052	(21)
Brown, *et al*., 1993	0.35215	(1)	0.30624	(5)	0.0035	(2)	0.0039	(3)
Maslen *et al*., 1993	0.35223	(4)	0.30622	(17)	0.0027	(1)	0.0029	(1)
Sawada, 1994	0.35217	(2)	0.30618	(8)	0.0032	(1)	0.0028	(1)

The best R_1 value for a single grain was 0.038. The R_1 for the merged set of the 17 grains was 0.034, but with much higher redundancy (14.5 as opposed to 3.6) and presumably better accuracy (within the assumption that the all grains are structurally identical). As can be seen in the table, the structural parameters derived from either the best grain, the various averages from the independent grain refinements, or the fully merged data are in good agreement with recent single crystal studies. The merged data set may have slightly better atomic displacement parameters. The treatment of the current data as a powder by averaging the raw data produces much worse results.

The refinement is reasonable, considering the nature of the data used. All of the parameters are within an acceptable range, except for the atomic displacement parameters, which are much too high. This is due to a poor signal to noise ratio at high Bragg angles leading to underestimates of the peak intensities.

The potential is clear: as long as the majority of the diffraction spots do not overlap with other spots any traditional single crystal refinement program can be applied and the results will be of the same quality. Hence, even solutions and refinements of complicated structures should be feasible. Furthermore, the method is independent of the size of the unit cell and, since many grains from the same sample are merged together, complete data sets may be collected by sampling only a small angular range, making the method well adapted for time-resolved studies or radiation sensitive samples.

Quantification of Minor Texture Components: Novel Recovery Mechanism During annealing of Deformed Aluminium Single Crystals

Recently, the 3DXRD methodology has been extended from the grain to sub-grain level [3] where it has been shown that the spatial resolving power is of the order of 0.03 μm^3. This opens the field of recovery and nucleation to in-situ studies. As a first application the microstructure within a 3D volume (0.2 x 0.2 x 2 mm^3) of a deformed Al single crystal was mapped before after annealing for 5 min at 300^{o}C. Cells or cell-blocks with

orientations far from those of the poles can be identified individually with a resolving limit of 0.3 μm. The diffraction pattern related to these tails of the orientation distribution changed drastically – despite the short annealing time - suggesting that the corresponding part of the microstructure is highly dynamic. Furthermore, on at least 3 occasions nuclei appeared with orientations that did not exist in the diffraction pattern of the as-deformed specimen. Hence, these nuclei appear to have formed either from rare cells with an initial size below the classical nucleation threshold or by a novel mechanism including rotation of the cells. These results contradict all existing models which assume that orientations within the deformed microstructure are conserved during annealing processes.

Risø 3DXRD Publications 1999-2001

[1] E.M. Lauridsen, D. Juul Jensen, H.F. Poulsen and U. Lienert. Scripta matter, **43**, p. 561-566 (2000).
[2] S.F. Nielsen, A. Wolf, H.F. Poulsen, M. Ohler, U. Lienert, and R.A. Owen. J. Synchrotron Rad., **7**, p. 103-109 (2000).
[3] H.F. Poulsen, D. Juul Jensen, T. Tschentscher, L. Wcislak, E.M. Lauridsen, L. Margulies, S. Schmidt. Textures & Microstructures, 35, 1, 39-54 (2001).
[4] L. Gottschalck Andersen and H.F. Poulsen (2001). Studies of High Temperature Superconductors **36,** Nova Science Publishers, New York, pp 29-87.
[5] H.F. Poulsen, N.H. Andersen, L.G. Andersen, and U. Lienert (2002). *Physica C* **370** , 141-145.
[6] U. Lienert, H.F. Poulsen, Å. Kvick. AIAA Journal, **39**(5), 919-923 (2001).
[7] U. Lienert, H.F. Poulsen, V. Honkimäki, C. Schulze, O. Hignete. J. Synchrotron Rad. **6** (1999) 979-984.
[8] E.M. Lauridsen, S.Schmidt, R.M. Suter, H.F. Poulsen. J. Appl. Crys. **34**, 6, 744-750 (2001).
[9] H.F. Poulsen, S.F. Nielsen, E.M. Lauridsen, S. Schmidt, R.M. Suter, U. Lienert, L.Margulies, T. Lorentzen, D. Juul Jensen. J. Appl. Cryst. **34**, 6, 751-756 (2001).
[10] L. Margulies, G. Winther, H.F. Poulsen. Science, **291**, 2392-2394 (2001).
[11] D. Juul Jensen, Å. Kvick, E.M. Lauridsen, U. Lienert, L. Margulies, S.F. Nielsen, H.F. Poulsen, Proc. of 5. MRS Fall meeting. Symposium R, Boston, MA (US), 29 Nov - 3 Dec 1999. Eds.: S.R. Stock, D.L. Perry, S.M. Mini. Materials Research Society Symposium Proceedings, **590,** 227-240 (2001).
[12] R.V. Martins, S. Grigull, M. Pinkerton, H.F. Poulsen, A. Kvick. Mat. Res. Soc. Symp. Proc, **590**, 241-246 (2000).
[13] S.F. Nielsen, W. Ludwig, D. Bellet, E.M. Lauridsen, H.F. Poulsen, D. Juul Jensen. Proc of 21st Risoe Int. Symp. On Mat. Science, 473-478 (2000).
[14] R.V. Martins, S. Grigull, U. Lienert, L. Margulies, A. Pyzalla. Proc. ICRS-6, Oxford, United Kingdom, **1**, 90 (2000).
[15] S. Schmidt, H.F. Poulsen, G.B.M. Vaughan. J. Appl. Cryst. In print.